Techno-Science Research Journal 11(2) (2023) 22-29

Content list available at ITC

Techno-Science Research Journal

Journal Homepage: www.ric.itc.edu.kh

Techno-Science Research Journal

Characterization Study of Cambodian Natural Rubber and Clay Composites for Shock Absorption Floor Mat

Laymey Sreng [1], Sirisokha Seang [1], Azura A. Rashid [2], Phanny Yos [1,3*]

[1] *Faculty of Geo-resources and Geotechnical Engineering, Institute of Technology of Cambodia, Russian Federation Blvd., P.O. Box 86, Phnom Penh, Cambodia*

[2] *School of Materials and Mineral Resources Engineering, Universiti Sains Malaysia, 14300 Nibong Tebal, Pulau Pinang, Malaysia*

[3] *Material Science and Structure Research Unit, Research and Innovation Center, Institute of Technology of Cambodia, Russian Federation Blvd., P.O. Box 86, Phnom Penh, Cambodia*

Received: 03 October 2022; Accepted: 25 April 2023; Available online: December 2023

Abstract: *Natural rubber is a polymeric material composed of hydrocarbon chains possessing high flexibility and green strength making them suitable for various applications including automotives tires, construction materials, and as floor protective materials etc. Special properties of rubber are obtained from compounding with various ingredients one of which is inorganic fillers including carbon black, silica, and clay minerals. The concept of processing techniques and optimization approaches has been studied for years but very few has explored the raw materials from Cambodia. In this work, the Cambodian natural rubber and clay filler from a local source will be studied for their combined characteristics as rubber composites for shock absorption floor mat application. The composites samples were produced via the conventional vulcanization system, incorporating clay filler at variation of 0, 5, 10, 15, and 20 part per hundred rubber (phr), and were analyzed on the physical, mechanical and impact properties, and morphology. The results showed that clay loadings at particle size range from 0.031 to 24.133 micrometer had trivial effects on rubber in terms of hardness and elongation at break. The swelling percentage has dropped significantly at high clay loading, reflecting an increase in crosslink density whereas rebound resilience received deteriorating effect from clay loadings due to partial distribution of micro-size clay particles. The tensile strength value of composites at clay loading 20 phr was reduced about 30% compared to the unfilled compound. The results were confirmed by the Scanning Electron Microscopic graphs showing filler pull-outs at tensile fracture surface as well as voids and some agglomerates acting as stress factors. However, rubber composites at 10 phr clay loadings showed superior properties on abrasion resistance index, at 15% higher than both the unfilled compound and composites at 20 phr whereas the impact energy absorption was about 10% higher. Compared to two types of commercial floor mats, the compounded composites showed superior performance in tensile properties and impact absorption ability.*

Keywords: Cambodian natural rubber; Common clay; Impact absorption properties, Aging, Rubber floor mat

1. INTRODUCTION

Natural rubber products have been circulating around our daily lives, for centuries, in forms of automotive parts, industrial equipment, household gadgets, footwear, and floor protection materials. Naturally, rubber contains various non-rubber constituents such as protein and phospholipids that attribute to its exceptional performance over a broad range of applications [1]. Due to increasing attention towards conscious resource consumptions while maximizing product performance, efforts have been made in optimizing the balance of rubber product quality and production cost, which have led to considerable amount of research studies exploring the effects of fillers incorporation in rubber. However, only few studies have looked into Cambodian natural rubber while in fact Cambodia was able to export over 366,000 tons of rubber in 2021, based on figures from the Ministry of Agriculture, Forestry and Fisheries. Natural rubber (NR) is an elastomeric hydrocarbon polymer yielded from the sap of rubber plants in the form of a milky emulsion known as latex. The milky sap contains primarily the latex and the non-isoprene components include proteins, carbohydrates, lipids, and inorganic constituents. Their presence is the main composition differentiating between natural rubber and synthetic rubber [2]. Furthermore, NR has the chemical structure of cis-

* Corresponding author: Phanny Yos
E-mail: phannyyos@itc.edu.kh; Tel: +855-12 870 256

1,4-polyisoprene that creates a phenomenon called strain-induced crystallization (SIC) in NR contributing to the outstanding properties of NR based products such as large elastic strain, high tensile strength, and a remarkable crack growth resistance [3], making them favorable for high performance applications. The transformation of raw NR into defined shapes and quality involves the vulcanization process where independent rubber chains are crosslinked by the reaction of sulfur with other ingredients under heat. Fillers are among the ingredients, incorporated to add weight to rubber compound. The most popular fillers include carbon black and non-black fillers such as clay, silica, and calcium carbonate etc. The processing techniques and the filler characteristics determine their roles in rubber matrix, which includes reinforcing, semi-reinforcing, and non-reinforcing. Within the conventional reinforcement system, clay that is added at micrometer size or relatively smaller [4] can create a polymer-filler bonding that in turn increases crosslink density of the materials hence improving stiffness and modulus. Moreover, clay is a rigid and inert filler material that occupies space in the matrix, further attributes to toughening elastomeric materials and overcoming poor processability, thus reducing production cost [2].

In addition to natural rubber resources, Cambodia is abundant with clay minerals mostly in the central region. However, their use is limited to the application of clay stoves and pottery products or fired bricks as construction materials. Because of their potentials in other useful applications, natural rubber and clay of local origin were utilized to produce rubber/clay composites. By focusing on the application of rubber shock absorption floor mat, this study will determine characteristics of the natural rubber and clay composites on properties such as hardness, swelling, crosslink density, tensile strength, elongation at break, rebound resilience, abrasion resistance, aging, impact energy absorption and scanning electron microscopy. The findings of the rubber composites properties will be then compared with commercial floor mats.

2. METHODOLOGY

2.1 Material preparations

Natural rubber (TSR 10) was obtained from Chub Rubber Plantation, Tboung Khmum province. The raw properties of TSR 10 include dirt 0.02%, ash 0.37%, volatile matter 0.30%, nitrogen 0.35%, initial plasticity at 40.8, plasticity retention index of 67.7, and 92.3 Mooney viscosity, ML(1+4) at 100 °C. Clay was taken from Prey Khmer Village, Kampong Chhnang province. Clay powder was prepared according to the ASTM D 2216 by drying in the oven at 105 °C for 24h then grinded and sieved for a diameter under 75 microns. The powder was dried for another 24h and subjected to dry milling for 24h to further reduce the particle size for better dispersion. Zinc oxide (ZnO) and sulfur were obtained from Xilong Co., Ltd. Stearic acid was supplied by Merck, Germany. 2-Mercaptobenzothiazole (MBT) and Tetramethylthiurum disulfide (TMTD) were purchased from Acros Organics. Phenolic Antioxidant (PA), was supplied by Rasching, Germany.

Two common types of commercial mats were purchased from local sport center and referred to as samples M01 and M02. Test specimen was cut from the rubber sheets into respective sample dimensions for the tests of swelling, crosslink density, hardness, tensile properties, aging, rebound resilience, and drop weight impact test.

2.2 Characterization of clay filler

The summary of clay characterization process is shown in Fig. 1. The chemical compositions were analyzed using X-ray Fluorescene Spectrometer (Rigaku ZSX PrimusIII). 5 g of clay powder was pressed following the method of flat type dies [5], while the particle size distribution was analyzed using Particle Analyzer (SALD 2300). The mineral elements of clay were determined by using X-ray diffractometer (Rigaku MiniflexII). Clay powder was dispersed in 200 ml distilled water and allowed for sedimentation. The clear solution obtained was then centrifuged at 150 rpm for 15 minutes. The particulates at the bottom of the cup were carefully extracted, put on glass plate and let dry for testing.

2.3 Composites compounding process

Following the conventional sulfur curing system, the compounding formulation in part per hundred rubber (phr) is shown in Table 1. The compounding process was carried out following ASTM D 3184 using a two-roll mill. The cure characteristics (ASTM D 2084) were carried out using Montech Moving Die Rheometer (MDR 3000) at 150 °C for scorch time (t_{s2}) and cure time (t_{90}). The compounds were vulcanized into composite sheets by a hot press molding machine at 150 °C and pressure of 1000 psi with the respective cure time t_{90}. Rubber/clay composites compound were signified as C0, C5, C10, C15, and C20 based on clay filler loadings.

Table 1 Compounding formulation for NR/clay composites

Reagents	Amount (phr)				
	C0	C5	C10	C15	C20
NR	100	100	100	100	100
ZnO	5	5	5	5	5
Stearic acid	2	2	2	2	2
Clay	**0**	**5**	**10**	**15**	**20**
MBT	1.5	1.5	1.5	1.5	1.5
TMTD	0.15	0.15	0.15	0.15	0.15
Antioxidant	1	1	1	1	1
Sulfur	2	2	2	2	2

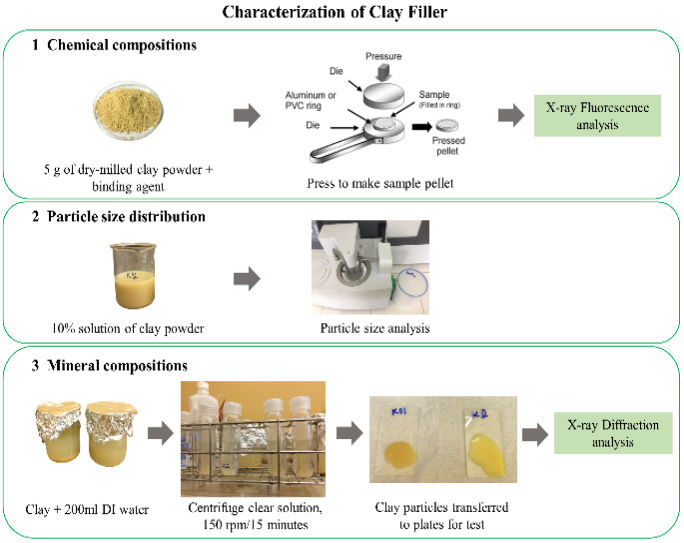

Fig. 1. Summary of clay filler characterization process

2.4 Crosslink density

The crosslink density was measured by the swelling method according to ASTM D 6814. The crosslink density was calculated using the Flory-Rehner equation in Eq. 1.

$$\nu_e = -[\ln(1 - V_r) + V_r + \chi_1 V_r^2]/[V_1(V_r^{1/3} - V_r)/2] \quad \text{(Eq. 1)}$$

where:

ν_e = the effective chain number in real network per unit volume (mol/cm^3)

χ_1 = the Flory-Huggins interaction parameter (toluene in cis-polyisoprene 0.391 at 25 °C)

V_1 = the molecular volume of solvent (toluene) 106.3 cm3/mol

V_r = the polymer volume fraction in a swollen network at equilibrium state, calculated following Eq. 2.

$$V_r = (W_D/D_D)/(W_D/D_D + W_{AS}/D_S) \quad \text{(Eq. 2)}$$

where:

W_D = the weight of dry rubber

D_D = the density of dry rubber

W_{AS} = the weight of the sample after dispersed in toluene

D_S = the density of toluene solvent.

2.5 Swelling test

Test specimen was cut from composite sheets and the commercial mats in dimension of 30 x 5 x 2 mm and immersed in toluene for 72 hours. The swollen specimen was taken out, gently wiped and weighted. Percentage of swelling is calculated following the ASTM D 471 as shown in Eq. 3.

$$\text{Swelling (\%)} = (M_2 - M_1)/M_1 \times 100 \quad \text{(Eq.3)}$$

where:

M_1 = the initial weight of the sample (g)

M_2 = the weight after immersion (g)

2.6 Hardness

Durometer Shore A was used to measure the sample hardness according to ASTM D 2240. The presser foot of the durometer was vertically pressed to samples of 6 mm thickness. Hardness values were taken from each sample at five different positions and the average was calculated.

2.7 Aging test

Aging test was carried out based on the ASTM D 573. Rubber composites and commercial mats were placed in the air oven (DRM620BD) at 105 °C for 24 h after which they were subjected to properties tests including hardness, tensile properties and tear strength. The obtained data was then compared with the unaged samples.

2.8 Tensile properties

Tensile properties including tensile strength and elongation at break were performed according to ASTM D 412 using the universal testing machine (LFM-TOP-50) at a crosshead rate of 500 mm/min. Test specimen was cut from composites sheets and commercial mats using dumbbell cutter Die C at dimension of 115 x 6 x 2 mm.

2.9 Rebound resilience test

Rebound resilience of rubber composites was studied using a Wallace Dunlop Tripsometer. The initial angle was set at 45° according to [6]. During test run, round test pieces of 6 mm was held in a vertical cavity. The pendulum was released from the initial angle to strike the test piece. Tests were conducted on three test pieces for each compound. The angle at which the pendulum rebound was taken for calculation of average and the percentage of rebound resilience was calculated.

$$\text{Resilience (\%)} = [(1 - \cos\theta_2)/(1 - \cos\theta_1)] \times 100 \quad \text{(Eq. 4)}$$

where:

θ_1 = the initial angle (45°)

θ_2 = the maximum rebound angle

2.10 Abrasion resistance index

Abrasion resistance of rubber composites was performed following BS 903-A9:1988, Method B. Rubber composites were molded into disc shapes and weighted. Each test consists of a trial run of 500 revolutions of the abrasive wheel followed by a running-in periods and five test runs according to the standard. After test stop, mass loss of samples after each test runs were

averaged for volume loss calculation. The result is expressed as abrasion resistance index as Eq. 5:

$$ARI = V_s / V_t \times 100 \quad \text{(Eq. 5)}$$

where:
V_s = volume loss of standard sample
V_t = volume loss of tested sample

2.11 Impact energy absorption

Impact energy absorption was conducted by ball drop impact test adapted from Amir et al. [7] by placing composites sheets on top of a ceramic floor tile of dimension 30 x 30 x 9 mm. A steel ball of 2.4 Kg was dropped onto the test pieces with increasing height until the floor tile breaks. The apparatus was assembled according to the ASTM F3007-13, in which the steel ball is dropped freely and impact the center of the specimen within 2 mm of center. The starting height was at 5.0 cm and was increased by 1.0 cm until floor tile breaks. Specimen was molded in dimension of 150 x 150 x 2 mm while the commercial floor mat was cut from sample sheets in the same dimension. During testing, samples thickness was adjusted to approximately 8 mm by stacking layers. A control was tested without rubber composites. The gravitational potential energy was calculated as illustrated in Eq. 6.

$$E = mgh \quad \text{(Eq. 6)}$$

where:
E = potential energy absorbed by composites (J)
m = mass of the ball weight (kg)
g = gravitational acceleration (9.81 m/s^2)
h = height (m), equals to the subtract of adjusted height by center of gravity of sphere mass.

2.12 Scanning electron microscope analysis

Tensile fracture surface of rubber composites was observed for its morphology under a scanning electron microscope, JOEL IT-500. Specimen was cut to small pieces of dimension 5.75 x 5.35 x 2 mm and sputter coated with platinum to increase thermal conduction and improve electron emission during observation. Unfilled rubber and composites of 10 and 20 phr clay concentrations were observed.

3. RESULTS AND DISCUSSION

3.1 Clay filler characteristics

Clay particle size result illustrated in Fig. 2 has showed a distribution range from 0.031 to 24.133 microns, suggesting that the preparation method of clay filler could partially produce a semi-reinforcing filler [8].The chemical compositions analysis is illustrated in Table 2 consists predominantly of silica (SiO_2) and aluminum oxide (Al_2O_3) at slightly above 54% and 26.92% w/w, respectively. The mineral groups of clay filler observed via X-ray diffraction analysis has shown diffraction peaks of two possible clay minerals such as Kaolinite with the spacing value of 7.15 and 3.57 Å, and Illite, which shows basal spacing of diffraction peaks at 9.9 – 10.1, 5.0, and 4.8 Å [9].

3.2 Cure characteristics and crosslink density of rubber/clay composites

The cure characteristics and crosslink density of NR/clay composites are expressed in Table 3. The result showed that cure time increased in the function of clay loadings. This has been commonly observed in clay-filled natural rubber composites as a result of the increment of silica content in the compound. Silica generally has a chemically reactive surface that usually adsorbs the ingredients used in accelerated sulfur curing system, which prolongs the cure time from 2 minutes to almost 4 minutes in t_{90}. Similar effect was reported by Bussaya & Wirunya [10] and Costa et al. [11] .

3.3 Swelling

The swelling percentage is shown in Fig. 3. Clay loading up to 10 phr had insignificant effect on swelling behavior while increment from 15 phr slightly decrease swelling percentage from 352% for unfilled compound to about 326% at clay loading 15 phr. This result could be due to clay particle dispersion and distribution within rubber matrix that helps reducing diffusion of solvent [12]. The result could be confirmed by the increase in crosslink density as shown in Table 3. Swelling of both commercial mats were significantly lower than rubber composites at about 128% and 119% for M01 and M02, respectively.

Table 2 Chemical composition of clay filler

Compositions	Weight (%)
SiO_2	54.3178
Al_2O_3	26.9291
Fe_2O_3	7.0012
K_2O	1.5737
TiO_2	0.6244
CaO	0.5697
MgO	0.4397
Na_2O	0.0941
ZrO_2	0.0408
Loss on ignition	8.2600

Table 3 Curing characteristics and crosslink density of rubber composites

Samples	Properties		
	t_{s2} (min)	t_{90} (min)	Crosslink density (x10^{-3} mol/cm3)
C0	1.06	2.11	8.94 (±0.00)
C5	1.34	2.61	8.95 (±0.00)
C10	1.63	2.91	9.02 (±0.00)
C15	1.74	3.20	9.43 (±0.00)
C20	1.86	3.75	9.44 (±0.00)

3.4 Hardness

Hardness values before and after aging of rubber in the effect of clay loadings and of commercial mats are illustrated in Fig. 4. Hardness value of NR composites varied between 39.7 to 40.1 Shore A, suggesting that composites received a trivial effect from clay loadings before aging even though there is a slight increase in the crosslink density. On the other hand, the hardness after aging was observed to have greater value than the unaged samples in the range of 44 to 46 Shore A. The increment is due due to the post-curing effect caused by thermal oxidation. This effect often causes chain scission of rubber chains and breaks the poly-sulfidic crosslinks produced from sulfur vulcanization into mono and di-sulfidic crosslinks, the types that deteriorate elasticity yet favor the stiffness of rubber composites [13]. As for commercial mats, M01 has the highest hardness value at 52 Shore A while M02 is on similar trend with rubber composites.

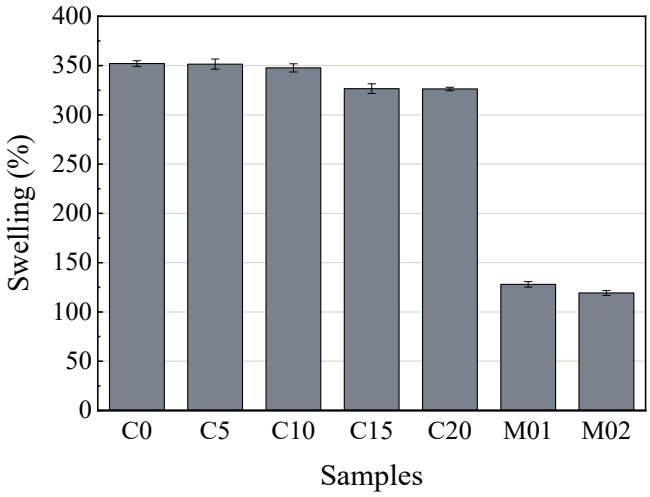

Fig. 3. Swelling percentage of samples C0, C5, C10, C15, C20, M01, and M02

3.5 Tensile properties

The tensile strength and elongation at rupture of rubber/clay composites and of commercial floor mats before and after aging are demonstrated in Fig. 5 and Fig. 6, respectively. Overall, the former graph shows a gradual drop in tensile strength in the function of clay loadings, whereas the latter shows that elongation at break merely fluctuated except for a slightly significant decrease at clay addition of 10 phr. At clay loading up to 20 phr, the tensile strength has reduced around 29 % compared to unfilled compound.

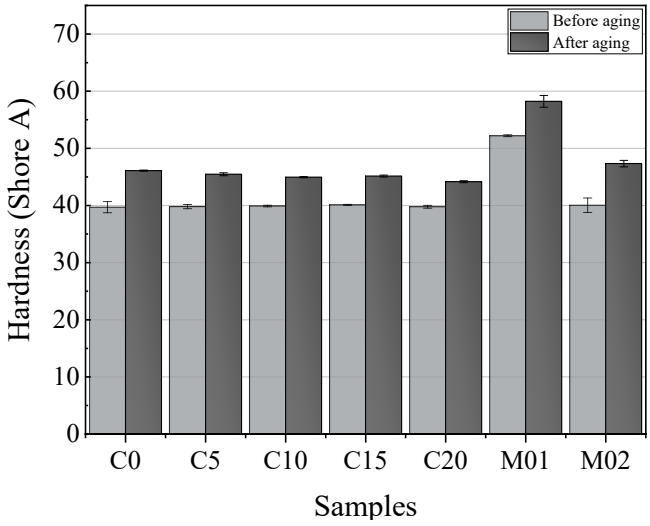

Fig. 4. Hardness of samples C0, C5, C10, C15, C20, M01, and M02 before and after aging

In agreement with the hardness results, this signifies that the clay filler could only add weight to rubber compounds while exhibiting no reinforcement on tensile properties of composites. Moreover, it has been reported that the increase of clay filler may lead to formation of filler cluster or agglomerates. In regards to the particle size result, the clay filler consists of large particles indicating small surface area. Therefore, when clay loading increases, the effective contact between filler and polymer matrix is compromised [14]. Consequently, natural rubber chains are difficult to rearrange and crystallize [15] and therefore become susceptible to stain deformation.

Regarding the graph after aging, thermal effect has evidently induced chain breakage in rubber composites, which drastically reduced tensile properties. However, clay loading at 20 phr could retain tensile properties slightly over 50%, indicating a good thermal resistance imparted by clay filler. With similar findings, some studies explained that clay could act as a good insulator and an essential barrier against moisture evaporation during heat aging [16], therefore, the deterioration effect on sample properties was reduced about 5 times compared to sample without clay. Both graphs further show that commercial floor mats exhibit significantly lower value of tensile properties at about 12 times and 9 times lower for M01 and M02, respectively, compared to rubber composites at the highest clay loadings.

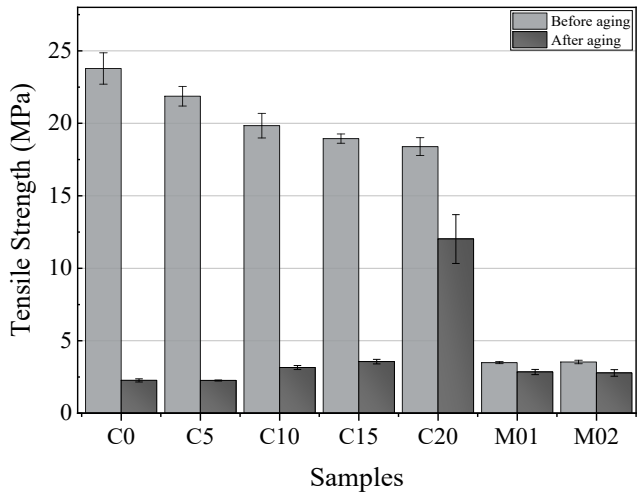

Fig. 5. Tensile strength of samples C0, C5, C10, C15, C20, M01, and M02 before and after aging

3.6 Rebound resilience

The percentage of rebound resilience of composites and commercial floor mats are shown in Fig. 7. Resilience values of composites up to 10 phr were insignificantly different while the value dropped from almost 86% at clay loading 10 phr to just below 79% at 20 phr. Resilience associates with hardness in that when hardness increases, resilience decreases. This small reduction in resilience is anticipated since the hardness results showed minimal changes. Evidently, rebound resilience of commercial mats is much lower than rubber composites due to more rigidity of the matrix.

3.7 Abrasion resistance index

The abrasion resistance index of rubber composites at 0, 10, and 20 phr of clay loading is illustrated in Fig. 8. In general, high abrasion resistance index of materials relates to great performance under abrasive or wearing environment. The graph shows that composites of 10 phr have the highest resistance index, approximately 15% higher than compound at 0 and 20 phr.

It has been claimed that good filler-rubber interfacial adhesion provides greater strength for composites against abrasion due to the formation of ridges on abraded surface that reduces contact area between abrader and rubber surface, preventing further abrasion [15]. Furthermore, the reduction in resistance of composites at higher clay loading could stem from poor filler dispersion and an increase in filler agglomerates.

3.8 Impact energy absorption

The maximum impact energy absorbed by rubber composites at clay loading of 0, 10 and 20 phr, and by commercial mats were compared in Fig. 9. The result shows that rubber composites at 0 and 20 phr could withstand impact about 2 times higher than control sample. Composites at 10 phr has the highest impact energy bearing capacity, approximately 9% better absorption compared to compound at 0 and 20 phr, and 19% higher than both types of existing commercial shock absorption mats. This finding corresponds with abrasion resistance index, suggesting that clay loading at 10 phr shows better properties in terms of wear resistance and impact absorption, due to the rigidity attribute from clay filler and good filler-rubber interactions.

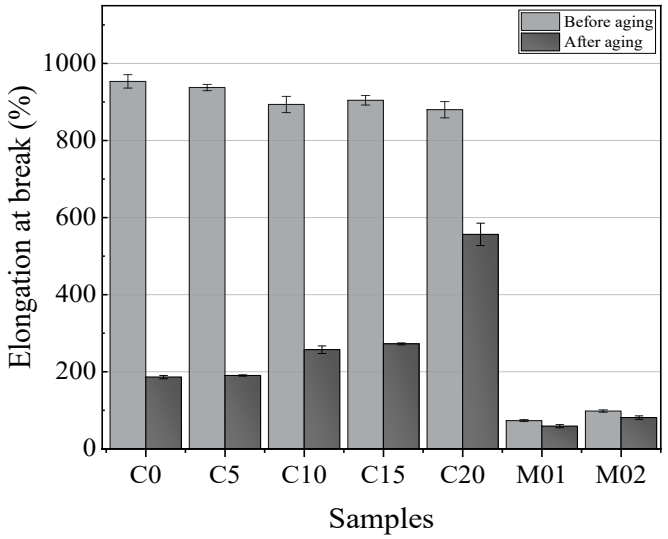

Fig. 6. Elongation at break of samples C0, C5, C10, C15, C20, M01, and M02 before and after aging

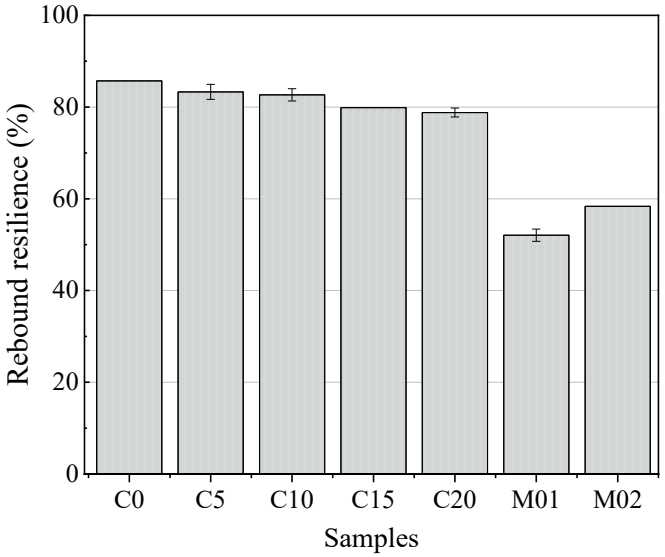

Fig. 7. Rebound resilience of samples C0, C5, C10, C15, C20, M01, and M02

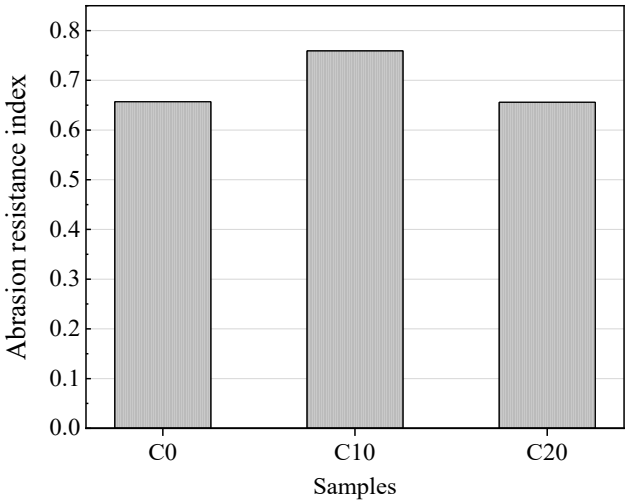

Fig. 8. Abrasion resistance index of rubber composites C0, C10, C20

3.9 Scanning electron microscopy

The morphology of rubber/clay composites at tensile fracture surface of (a) C10 and (b) C20 are demonstrated in Fig. 10. at capturing scale of 100 micrometers. For both samples, many undispersed filler particles can be observed as a result of an inhomogeneous blending of clay filler and rubber.

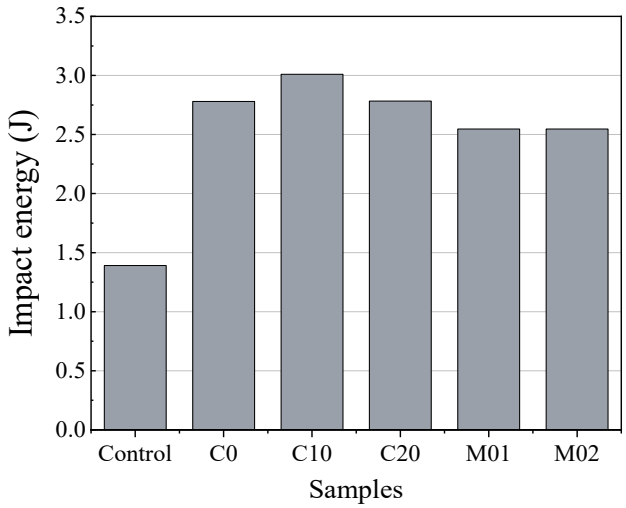

Fig. 9. Impact energy absorption of samples C0, C10, C20, M01, M02

Due to its rigid nature and large particle size, clay filler did not adhere well to rubber matrix, leading to filler pull outs and voids on the surface that could create stress points for fracture initiation. From the mechanical properties results, sample C10 demonstrated better properties than C20 due to less filler clusters. As seen in the graph, clay filler formed agglomerates in addition to a high ratio of particles that densely filled up the entire surface. Such interaction indicates poor strain properties of rubber composites, which explains the reduction in tensile strength, elongation at break, and rebound resilience as clay loading increased.

(a)

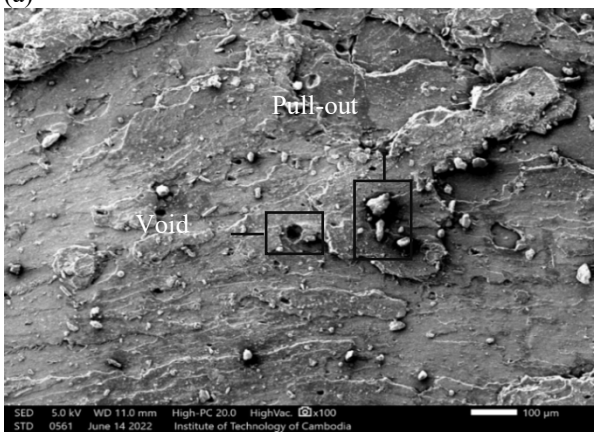

(b)

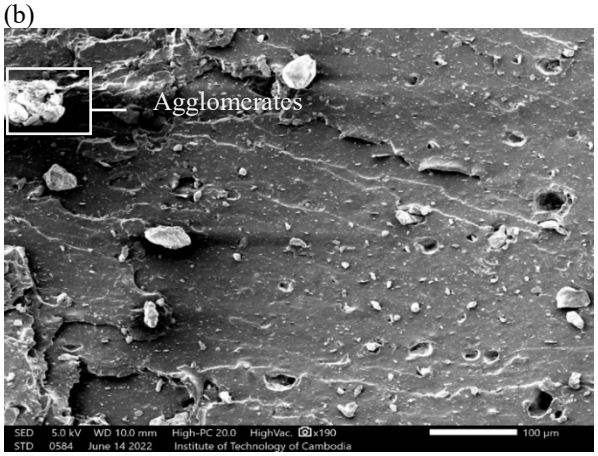

Fig. 10. SEM of composites sample (a) C10 and (b) C20

4. CONCLUSIONS

In this study, rubber and clay composites were produced by compounding natural rubber with clay filler. The composites were tested for physical, mechanical, impact properties and morphology; and comparison was made with commercial floor mats. Overall results showed that the composites are superior to commercial mats in shock absorption and tensile properties but inferior in hardness. The NR composites at clay loading 10 phr could absorb about 19% higher impact energy while clay loading 20 phr had tensile properties values about 10 times higher compared to both types of commercial mats. Clay loadings up to 20 phr had insignificant effects hardness and elongation at break. The tensile strength before aging was reduced with clay loadings but after aging, composites at 20 phr has retained properties more than 50% indicating better thermal resistance. A positive attribution from clay was observed at 10 phr for abrasion resistance and impact energy absorption due to good filler-rubber interaction unlike composites at highest clay loadings,

which consist of more filler agglomerates as seen by the SEM micrographs. The remarkable difference in tensile properties of NR and clay composites at 20 phr along with its thermal resistance ability compared to the commercial mats, signified a scope for development. Future work will be established to examine composites at higher clay loadings and compare with standard grades of shock absorption floor mats.

ACKNOWLEDGMENTS

The work was funded by Cambodia Higher Education Improvement Project (Credit No. 6221-KH). The experimental facilitation provided by the Institute of Technology of Cambodia (ITC), School of Materials and Mineral Resources Engineering of Universiti Sains Malaysia (USM) and the Cambodian Rubber Research Institute (CRRI) was gratefully acknowledged.

REFERENCES

[1] Nussana, L., Akarapong, T., Ladawan, S., Nattapon, U., Karnda, S., Jobish, J., Yeampon, N., & Ekwipoo, K. (2022). Influence of Non-Rubber Components on the Properties of Unvulcanized Natural Rubber from Different Clones. Polymers, 14, 1759.

[2] Liliane, B. (2018). Natural rubber Nanocomposites: A Review. Nanomaterials, 9, 12.

[3] Huneau, B. (2011). Strain-induced crystallization of natural rubber: A review of X-Ray diffraction investigations. Rubber Chemistry and Technology, 84, 425-452.

[4] Azemi, B. S. (2013). Theory and Mechanisms of Filler Reinforcement in Natural Rubber. Natural Rubber Materials, Volume 2, 73-165.

[5] Gakuto, T. (2015). Sample preparation for X-ray fluorescence analysis. Rigaku Journal, 31(1), 26-30.

[6] Ismail, H., Ahmad, H. S., & Rashid, A. A. (2015). Fatigue, resilience, hardness, and swelling behaviour of natural rubber/recycled NR/NBRr blends. Polymers and Polymer Composites, 23, 583–588.

[7] Amir, N., Hisham, M., & Abidin, K. A. Z. (2018). Study of Physical Properties and Shock Absorption Abilities of Starch Polymer Foam as Cushioning Material for Packaging. MATEC Web of Conferences, 225.

[8] Azura, A. R., & Siti, R. Y. (2013). Mechanical Properties of Natural Rubber Composites Filled with Macro- and Nanofillers. Natural Rubber Materials, Volume 2, 2: 550–573.

[9] Chen, P. Y., 1977. Table of Key Lines in X-ray Powder Diffraction Patterns of Minerals in Clays and Associated Rocks. Department of Natural Resources Geological Survey Occasional Paper, 21.

[10] Bussaya, R. & Wirunya, K. (2007). The Development of Rubber Compound based on Natural Rubber (NR) and (EPDM) Rubber for Playground Rubber Mat. Natural Sciences, 41, 239–247.

[11] Costa, D. H. M., Visconte, L. L. Y., Nunes, R. C. R., & Furtado, C. R. G. (2003). Partial replacement of commercial fillers and the effect on the vulcanization process. Journal of Applied Polymer Science, 87, 1405–1413.

[12] Do, Y. K., Jae, W. P., Dong, Y. L., & Kwan, H. S. (2020). Correlation between the crosslink characteristics and mechanical properties of natural rubber compound via accelerators and reinforcement. Polymers, 12, 1–14.

[13] Lee, K. C., Yusoff, N. A. M., Othman, N., & Mohamad Aini, N. A. (2017). Effect of vulcanization temperature on curing characteristic, physical and mechanical properties of natural rubber/palygorskite composites. IOP Conference Series: Materials Science and Engineering, 223, 1–11.

[14] Frölich, J., Niedermeier, W., & Luginsland, H. D. (2005). The effect of filler-filler and filler-elastomer interactioin on rubber reinforcement. Composites: Part A, 36, 449-460.

[15] Junkong, P., Kueseng, P., Wirasate, S., Huynh, C., & Rattanasom, N. (2015). Cut growth and abrasion behaviour, and morphology of natural rubber filled with MWCNT and MWCNT/carbon black. Polymer Testing, 41, 172–183.

[16] Kiliaris, P., & Papaspyrides, C. D. (2010). Polymer/layered silicate (clay) nanocomposites: An overview of flame retardancy. Progress in Polymer Science, 35, 902–958.